LIM: OPTIMIZATION OF SECONDARY WIDTH RESPECT TO THE THRUST

(*) G. D'Ovidio, (**) F. Crisi, (**) A. Navarra, (***) M. Villani, (*) G. Lanzara

(*) Transportation Department, University of L'Aquila, 67040, Poggio di Roio (I)
Phone: +39-0862-434106 Fax: +39-0862-434143; e-mail: dovidio@dau.ing.univaq.it
(**) Science and Technology Park of Abruzzo, Via Antica Arischia, 1, 67100 L'Aquila (I)
Phone: +39-0862-3475311 Fax: +39-0862-3475210; e-mail: trasporti@pstabruzzo.it
(***) Dept. of Electrical Engineering, University of L'Aquila, 67040, Poggio di Roio (I)
Phone: +39-0862-434419 Fax: +39-0862-434403; e-mail: villani@ing.univaq.it

Keywords

Electromagnetic way, finite element analysis, levitation.

Abstract

The paper deals with the investigation of the optimal width of the secondary in a Linear Induction Motor, respect to the primary dimensions, with reference to the thrust and levitation. An experimental equipment has been designed and built that reproduces on small-scale the motion of vehicle along an electromagnetic way.
Significant experimental tests have been carried out in order to characterize the circular inductor way with annulus-type secondary and evaluate the effect of several parameters on the performance.
Moreover, an accurate 3-D Finite Element model has been carried out and the simulation results have been compared with the experimental ones. This model has allowed to optimize the secondary width in order to maximize the thrust.
This study should bear gradually the construction of an equipment with high-temperature superconducting materials

1 Introduction

Preliminary analyses [1,2] on the use of superconducting sheets for magnetic levitation have pointed out that the intensity of pressures, both levitation and traction, were widely compatible with transportation applications [3].
Starting from the simulation results, the authors have designed and built a first experimental equipment that reproduce on small-scale the "vehicle-track" system in both static and dynamic conditions.
This equipment has allowed to begin the experimental tests that should bear gradually the construction of an equipment with superconducting materials, and for this reason the following steps have been scheduled with reference to the nature and shape of the conductor in the secondary:

1st) Disc with ordinary conductor sheets in aluminum; this solution has been already studied in [4];
2nd) Annulus with ordinary conductor sheets:
3rd) Annulus consisting of separate sectors with ordinary conductor sheets;
4th) Superconducting sheets

In this paper the 2nd step has been investigated and the experimental results related to this step are presented and discussed.
These results have stimulated the authors to analyze deeply the interaction between the electromagnetic way and the annulus-type secondary by means of an accurate 3-D Finite Element models that has been tuned thanks to the experimental results.
The availability of an accurate 3-D model has allowed to investigate the effects of the annulus width on the thrust vs. slip characteristic, in order to find the optimal solution.

2 Description of the experimental equipment

Instead of realize a linear machine of finite dimension, a circular equipment has been built that consists of two main parts:

a) a circular inductor that represents the primary and simulates the track; it can rotate around its vertical axis:
b) an annulus-type secondary, that simulates the vehicle, realized by multi-layers aluminum and a ferromagnetic steel.

The ferromagnetic core of primary has been made by winding a 0.5 mm non-oriented electrical steel sheets up to obtain a circular ring of 41 mm thickness. Then, this ring has been milled accurately to realize rectangular slots. The secondary consists of a steel annulus to which aluminum sheets are assembled. The design data of the experimental equipment are presented in Tab.1, while Fig.1 shows a general view of experimental equipment.

The ferromagnetic core has been coupled with an a.c. machine, fed by three-phase Inverter: both static and dynamic tests have been carried out.

The equipment simulates by analogy the behavior of a vehicle with a conducting sheets that moves along an "electromagnetic way". For convenience, the tests have been carried out by locking the secondary and leaving the primary free to rotate.

The interaction between the primary and secondary has been evaluated by a torquemeter and a load cell, that is a bonded strain gauge force transducer. Since the variations in strain are dynamic, the bridge circuit is operated in the unbalanced condition, e.g. an output proportional to the variation in resistance of the active gauge is obtained.

The speed of primary can be controlled by the coupled motor and all the operating conditions have been tested.

Table 1: Design data of the experimental equipment

number of poles		12
number of slots		36
Primary:		
laminated core thickness	(mm)	41.0
slot width	(mm)	17.9
slot high	(mm)	33.3
air-gap	(mm)	5 ÷ 25
conductors per slot		200
Secondary		
Annulus width (in Al)	(mm)	41 - 82
annulus thickness (in Al)	(mm)	6.5
thickness of ferromagnetic steel	(mm)	4.0

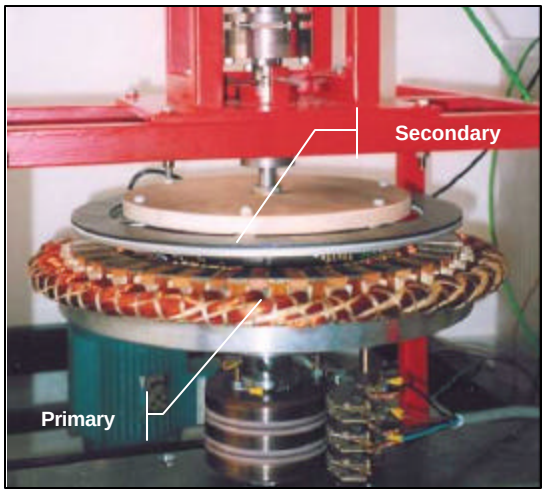

Fig. 1- General view of the experimental equipment

3 The experimental results

Significant experimental tests have been carried out in order to characterize the equipment and evaluate the effect of air-gap length and phase voltage, on the torque and normal thrust.

3.1 The torque

In Fig.2 are shown the Torque-slip curves for different air-gap lengths related to 6.5 mm aluminum thickness, 4 mm ferromagnetic steel and a phase voltage in the range 100÷150 V (50 Hz). For these tests the secondary width is equal to the inductor one.
The air-gap reduction gives rise significant torque increases in all operating conditions, for both voltage levels: e.g. the torque with an air-gap of 10 mm is double respect the 20 mm air-gap one.
The above mentioned figures point out how, for an air-gap of 5 mm, the torque assumes a negative value at synchronous speed (500 rpm): this behavior is due to the presence of the 5th harmonic in the magnetic flux density in the air-gap (due to the slotted primary) that gives rise to a parasitical breaking torque. The entity of this torque is sufficient to balance the main torque when the speed is close to synchronism. The effect of this harmonic is negligible for higher air-gap, but for small air-gap it is substantial.

Further tests have been carried out removing the ferromagnetic steel in the secondary, in order to evaluate the effect on the torque and normal thrust: the torque vs. slip curves are shown in Fig.3 and point out a drastic torque reduction respect to the previous results.

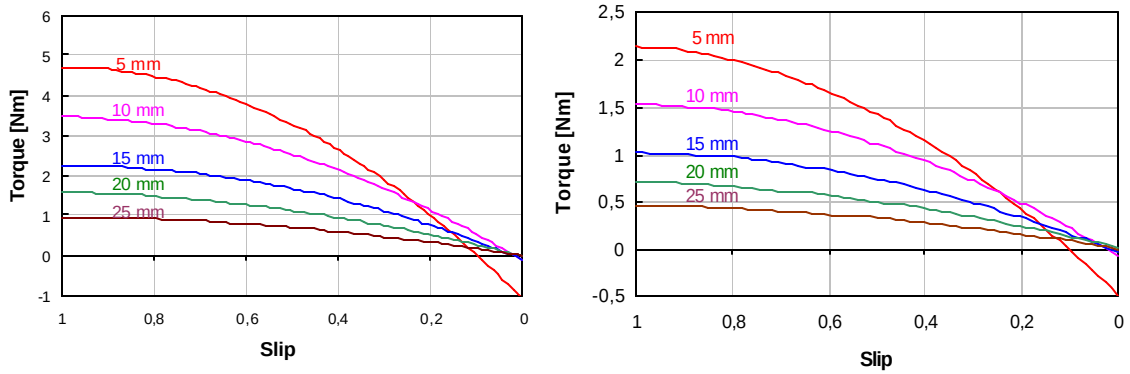

Fig. 2 – Torque Vs. slip for different air-gap lengths (Al = 6.5 mm; Fe = 4 mm).
a) 150 V; b) 100 V.

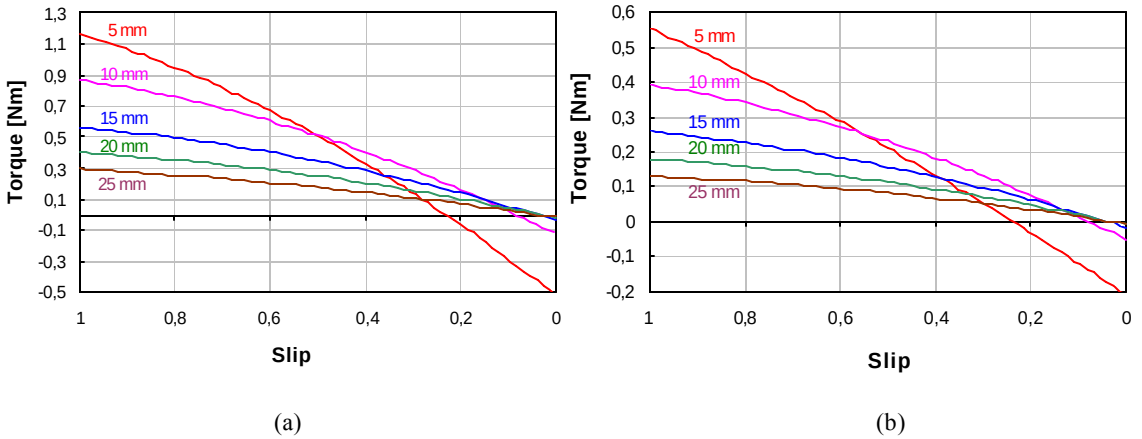

Fig. 3 – Torque Vs. slip for different air-gap, without ferromagnetic steel in the secondary (Al = 6.5 mm).
a) 150 V; b) 100 V.

3.2 The normal thrust

Interesting tests have been carried out for the normal thrust evaluation in the secondary: the behaviors are shown in Fig. 4.

In the case of a multi-layer secondary containing a ferromagnetic core, the normal thrust depends on the difference of the attractive force (between the primary and secondary) and the electrodynamics repulsive force due to the action of the eddy currents induced in the secondary conductor on the primary magnetic field. For a non-ferromagnetic secondary the force repels the secondary from the primary core.

In Fig.4a the thrusts are obviously attractive for the presence of the ferromagnetic steel in the secondary, and the entity is significant when the air-gap reduces: for an air-gap of 10 mm the thrust is 5 times higher the thrust with 25 mm.

When the ferromagnetic steel is removed, the normal thrusts are repulsive (Fig.4b) with low values respect to the previous results.

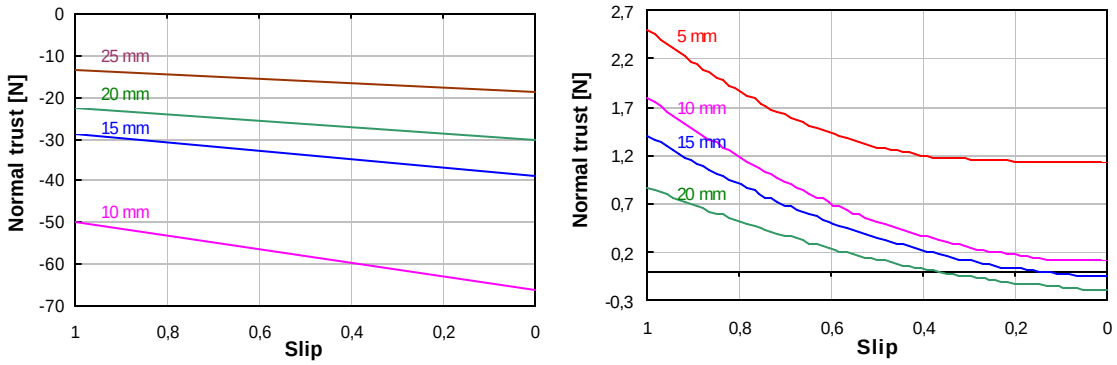

(a) (b)

Fig. 4 – Normal thrust Vs. slip for different air-gap lengths
a) Al = 6.5 mm, Fe = 4 mm, 150 V; b) Al = 6.5 mm, 150 V.

4 The 3-D Finite Element model

In order to investigate deeply the interaction between the electromagnetic track and the annulus-type secondary, an accurate 3-D Finite Element model has been carried out and several geometric variables has been introduced that have allowed to evaluate their effects on the motor performance.

This model has been tuned starting from the experimental results of the previous analysis. It has allowed to investigate not only the interaction between the primary and secondary, but also to find the optimal annulus width that maximizes the torque.

The unconventional structure of equipment has required a 3-D Finite Element model in order to take into account the non-linear iron behavior and saturation effects. The Figures 5 and 6 show respectively the 3-D mesh and a cross section of the equipment, while Fig.7 presents the flux density in the core of primary.

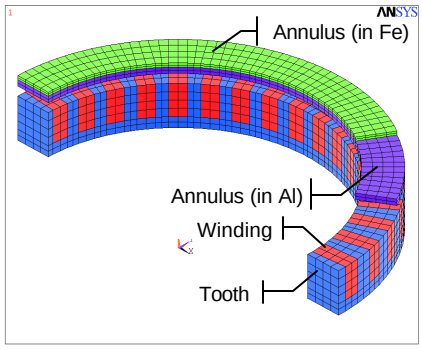

Fig. 5 - 3-D mesh of the experimental equipment

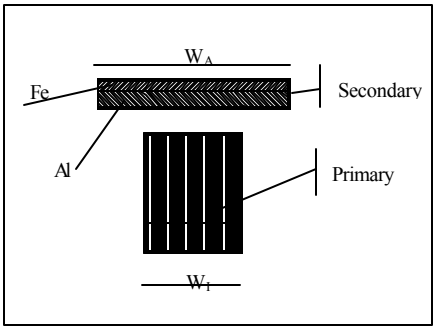

Fig. 6 - Cross section of the equipment

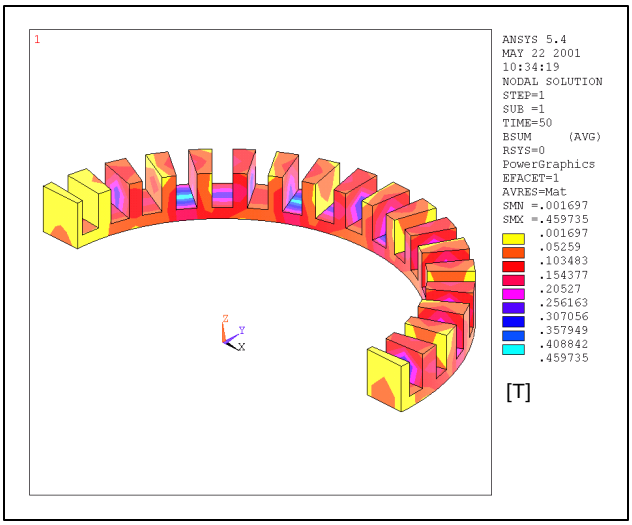

Fig. 7 - Flux density in the core

The FE model has been refined by means of the previous experimental tests. The comparison between simulation and experimental results is shown in Fig.8 and confirms the accuracy of the model.
The model has allowed to evaluate the flux density and the eddy current distribution in the secondary with reference to two different operating conditions: at standstill and at synchronous speed. The Fig.9a, 9b and Fig.10a, 10b show these maps in detail with reference to a secondary width equal to core thickness and an air-gap of 10 mm.
The comparison of the eddy currents point out significant differences not only on the values but also on the path. At standstill operation the entity of currents is higher and the currents close after one pole pitch (τ). At synchronous speed, the eddy currents are very low and they are due to the presence of the 5^{th} harmonic in the magnetic field: in this case the path length correspond approximately to a slot pitch (τ_S).

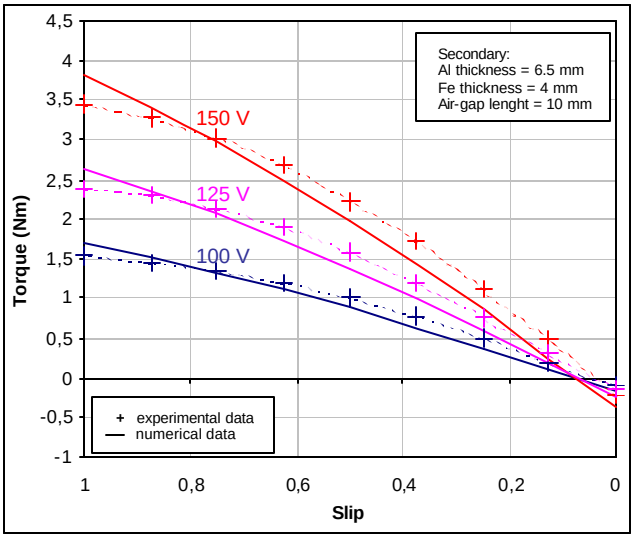

Fig. 8 - Torque vs. slip: comparison between simulation and experimental results

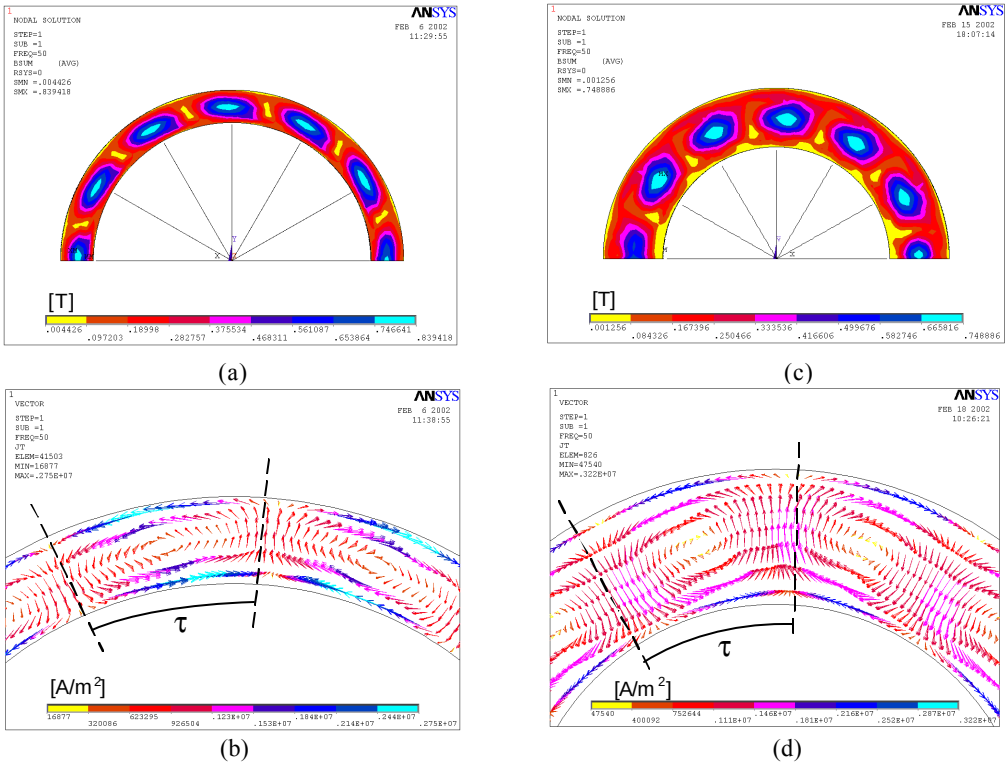

Fig. 9 – Standstill operation: Flux density in the Fe (a, c); eddy current distribution in the Al (b, d)
a, b) secondary width equal to core thickness
c, d) secondary width 2 times larger the core thickness

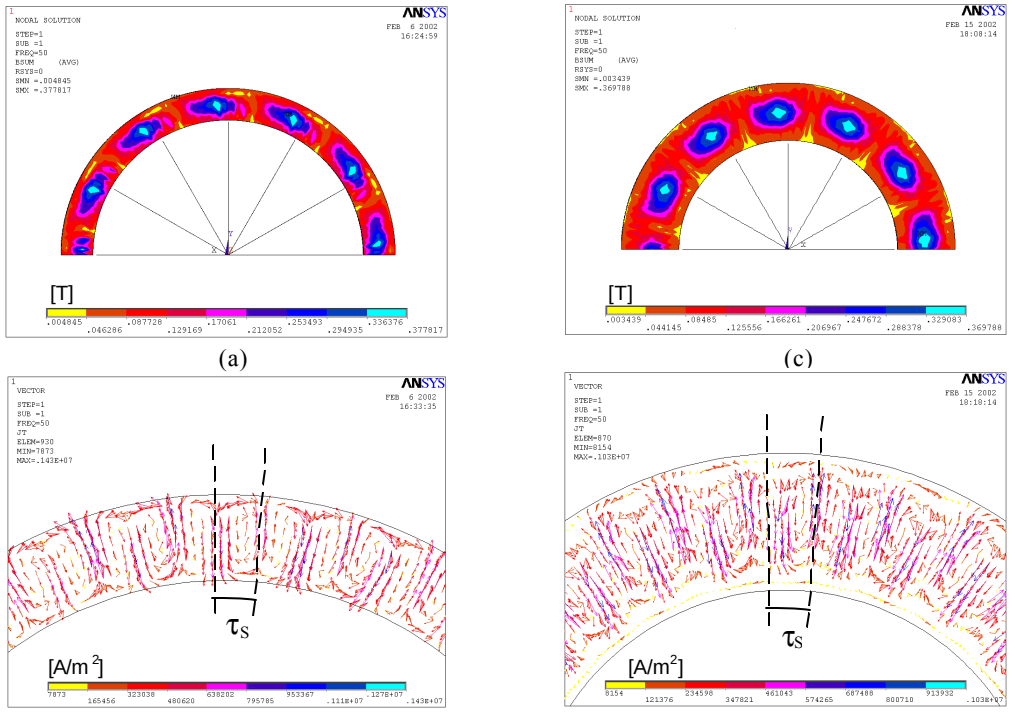

Fig. 10 – Synchronous speed: Flux density in the Fe (a, c); eddy current distribution in the Al (b, d)
a, b) secondary width equal to core thickness
c, d) secondary width 2 times larger the core thickness

The availability of an accurate 3-D model has allowed to investigate the effects of the secondary width on the thrust-slip characteristic, in order to find the best solution. A parameter (k) has been introduced that represent the ratio between the laminated core thickness W_I and secondary width W_A (Fig.6).
The curves shown in Fig. 11 and 12 present the thrust vs. slip and the "thrust per unit area of secondary" vs. slip characteristics for different k values. Particularly, the thrust per unit area represents the ratio between the torque and the average radius of the secondary (0.195 m).
The lower torque values correspond to k equal 1 (that is the secondary width equal to core thickness), and this trend is worst respect to the disc-type secondary one [4].
Further improvement has been achieved by reducing k, and this has produced also a significant increase on starting thrust. A further reduction below 0.5 does not give rise any profitable and the curves tend to coincide: in fact, if the secondary width is very large, the external area is not involved by the main flux and does not affect significantly the traction values.
The results of this analysis suggest to choice k in the range 0.5÷0.6, that is the secondary width should be about 1.6 ÷ 2 times larger the inductor thickness.
A 3-D Finite Element analysis has been carried out with a secondary width 2 times larger the core thickness (k=0.5). The flux density distributions in the ferromagnetic steel are shown in Fig.9c and 10c, while Fig.9d, 10d present the eddy current in the aluminum at standstill and synchronous speed. The comparison with Fig.9b and 10b points out a different distribution of currents that reflects on the current values.
About the thrust per unit area of secondary (Fig. 12), it is evident how a right choice of the k value gives significant thrust increases: for a slip less than 0.7 the optimal k value is 0.6 while, for an operation close to standstill, a value equal to 0.5 is more suitable.

Conclusions

The authors have designed and built a first experimental equipment, that reproduce on small-scale the "vehicle-track" system in both static and dynamic conditions: it consists of a circular inductor "way" with annulus-type secondary.
Experimental tests have been carried out in order to evaluate the entity of traction force and normal thrust for different air-gap lengths and phase voltage.
These results have allowed to carried out and tune a 3-D Finite Element model in order to investigate deeply the interaction between the track and the secondary. Moreover, the availability of an accurate model has allowed to investigate the effects of the annulus width on the motor performance, to find the best solution in terms of thrust.

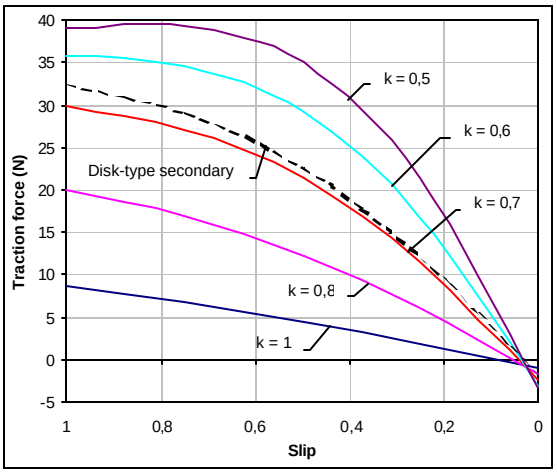

Fig. 11 - Thrust vs. slip for different k values

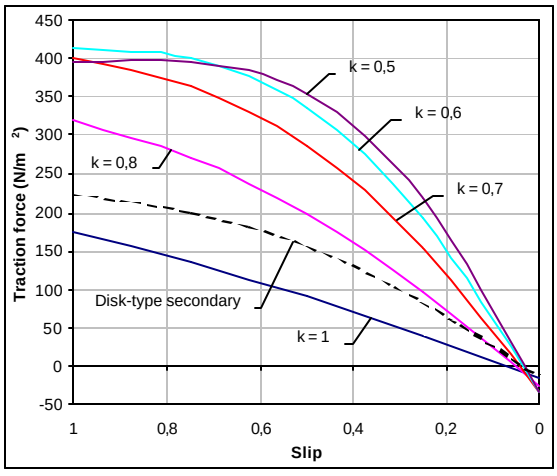

Fig. 12 – Thrust per unit area of secondary vs. slip for different k values

6 References

1. G. Lanzara, G. D'Ovi dio, C. Masciovecchio, M. Villani. *Superconducting Sheets for Train Support and Traction : Finite Element Analysis*, IEEJ -LDIA'98,Tokyo, Japan, 1998.
2. G. Lanzara. *Magnetically levitated vehicle with superconducting mirror sheets interacting with guideway magnetic fields*, U.S. Patent n°. 4,797,445 1990.
3. J. F. Gieras. *Linear Induction Drives* , Clarendon Press, Oxford, 1994.
4. G.D'Ovidio, G.Lanzara, F.Crisi, A.Navarra, M.Villani. *Circular inductor "way" with disc-type secondary: experimental equipment and characterization*, IEEJ - LDIA'01, Nagano, Japan, 2001.